

A. GRAJCAR*, B. GRZEGORCZYK*[#], M. RÓŻAŃSKI**, S. STANO**, M. MORAWIEC***MICROSTRUCTURAL ASPECTS OF BIFOCAL LASER WELDING OF TRIP STEELS**

This work is concerned with comparative tests involving single-spot and twin-spot laser welding of thermomechanically rolled TRIP steel. The welding tests were carried out using keyhole welding and a solid state laser. In the case of twin-spot laser beam welding, the power distribution of beams was 50%:50%. The changes in macro- and microstructures were investigated using light and scanning electron microscopy. Three main zones subjected to the tests included the fusion zone, the heat affected zone and the intercritical heat affected zone (transition zone between the base material and the HAZ). Special attention was paid to the effect of various thermal cycles on the microstructure of each zone and on martensite morphology. The tests involved hardness measurements carried out in order to investigate the effect of different microstructures on mechanical properties of welds.

Keywords: TRIP steel, retained austenite, dual beam, laser welding, AHSS, hardness profile

1. Introduction

Laser welding is one of the most popular techniques used when joining car body elements [1]. This technology is continuously developed in order to improve the properties of welded joints [2]. One of the latest laser welding techniques utilises a split laser beam enabling welding by means of two or more laser beams. Multi-beam laser welding can be conducted using two laser heads or a special optical module [3]. Presently, twin-spot laser welding is tested in relation to joining galvanised sheets [4] or light metal alloys [5,6]. Important materials for the automotive industry include advanced high strength steels (AHSS), i.e. DP, CP and TRIP steels [7-13]. Their practical use depends, among other things, on weldability [14,15].

Recently, Grajcar et al. [15,16] have been testing the conventional laser welding of TRIP steels using a single-spot beam. They have also tested the effect of welding parameters on the presence of non-metallic inclusions in the fusion zone of welded joints [17]. Advanced High Strength Steels, particularly those characterised by significantly high strength tend to be problematic during welding. Górka [18] reported that the weakest area, as regards the welding of high-strength steels containing microalloyed elements, was a coarse-grained heat affected zone (HAZ). Such a situation is caused by the uncontrolled precipitation of carbonitrides or due to the “softening” of the HAZ.

Twin-spot laser welding makes it possible to improve the quality of welded joints by controlling the dynamics of welding thermal cycles. This technique enables performing welding processes with the double melting of the weld material and heat

treatment preceding or following welding processes. However, when welding TRIP steels containing microadditions such as Nb and Ti, it is necessary to pay special attention to the uncontrolled precipitation of carbonitrides in the material of the joint. This is particularly important in cases of processes characterised by complicated thermal cycles and requires the extensive knowledge of the kinetics of carbonitride precipitation in steels [19].

2. Material test

The objective of the research involved comparative tests of the single and twin-spot laser welding of TRIP steel. In both cases the same material was used, i.e. a 2 mm thick and 100 mm wide steel sheet. The steel was obtained in the thermo-mechanical process with controlled cooling directly from the finishing hot rolling temperature. In order to stabilise retained austenite, the material was held at the temperature of 350°C for 600 seconds. The chemical composition of the steel is presented in Table 1.

TABLE 1

Chemical composition of the tested steel

| C | Mn | Si | S | P | Nb | Ti | N | Al | C _{eq} |
|------|------|------|-------|-------|-------|-------|--------|------|-----------------|
| 0.24 | 1.55 | 0.87 | 0.004 | 0.010 | 0.034 | 0.023 | 0.0028 | 0.40 | 0.54 |

Due to the negative influence of silicon on hot-dip galvanising processes, its content was reduced in the steel subjected to the tests. However, silicon prevents the precipitation of car-

* SILESIAAN UNIVERSITY OF TECHNOLOGY, INSTITUTE OF ENGINEERING MATERIALS AND BIOMATERIALS, 18A KONARSKIEGO STR., 44-100 GLIWICE, POLAND
 ** INSTITUTE OF WELDING, 16-18 BL. CZESLAWA STR., 44-100 GLIWICE, POLAND

[#] Corresponding author: barbara.grzegorzczuk@polsl.pl

bides during bainitic transformations, enabling the enrichment of retained austenite in carbon and, as a result, increasing its temperature stability [10,20]. Due to the foregoing, the steel was provided with an addition of aluminium which also prevents the precipitation of carbides, yet unlike silicon, does not affect the process of hot-dip galvanising.

3. Methodology

The single and twin-spot welding tests involving TRIP steel were performed using a robotic system for laser processing, integrated with a solid state laser and meeting the requirements of the most advanced industrial stations. The system was equipped with:

- laser TruDisk 12002-a Yb:YAG solid-state laser,
- CFO head (Trumpf) used for single-spot laser welding,
- D70 head (Trumpf) enabling twin-spot laser welding,
- UFF100 laser beam analyser (Prometec).

Detailed information about components of the welding station can be found in articles [15,16]. Welding was performed in air atmosphere. Table 2 presents welding parameters in relation to individual processes.

TABLE 2

Welding parameters of single and twin-spot welding

| Specimen designation | 1 | 2 | 3 | 4 |
|----------------------------|-------|-------|-------|-------|
| Total beam power, kW | 2 | 4 | 6 | 4 |
| Beam power distribution, % | — | — | 50:50 | 50:50 |
| Welding rate, m/min | 2.5 | 4.5 | 7.5 | 4 |
| Linear energy, kJ/mm | 0.048 | 0.053 | 0.048 | 0.060 |
| Atmosphere | Air | Air | Air | Air |

The total beam power and welding rate were adjusted in a manner enabling the entire penetration of the material being welded. The twin-spot laser beam is obtained by placing a special optical module across the laser beam, thus changing its trajectory. Afterwards, the beam is focused on two spots by standard focusing lenses. The distance between the focuses of the laser beam is affected by the inclination of the optical module plane. The laser beam power distribution is influenced by the position of the optical module in relation to the laser beam. The maximum distance between the beam focuses adopted when making the test joints amounted to 4 mm. Twin-spot laser welding was performed with the beam power distribution of 50:50, in the tandem system. The above-presented parameters enabled the remelting of the material subjected to welding.

The preparation of specimens for macro- and microscopic metallographic tests as well as hardness measurements involved the cutting of the welded joints in the plane perpendicular to the weld axis. The specimens were included in epoxy resin, subjected to grinding by means of abrasive paper having a granularity of 80, 320, 1000 and 2500 and next to polishing by means of initially diamond and next corundum slurry, having grain sizes of 3 μm

and 0.05 μm respectively. The microstructure of the specimen was revealed by etching in 3% Nital and in the aqueous solution of sodium pyrosulfate. The metallographic specimens prepared in the manner described above were subjected to macro- and microscopic examinations. The macroscopic tests, performed using an MeF4 light microscope (Leica), aimed to identify the macrostructure and geometrical dimensions of the welded joint. In turn, the microscopic observations aimed at the identification of structural constituents in the microstructure of the fusion zone, in the HAZ and in the transition zone between the base material and the HAZ. In addition, the microscopic identification was performed using a SUPRA 25 scanning electron microscope in the BSE observation mode.

4. Results and Discussion

4.1. Geometry of the joint

The first stage of investigations involved the macroscopic observation of the welded joints (Fig. 1). The observation revealed that the macrostructure of the welded joints was composed of columnar crystals oriented in parallel to the direction of the fastest cooling, visible particularly well in Figure 1c and 1d. The macroscopic observation also revealed that the face and the root of the weld obtained in twin-spot welding were characterised by better quality than those obtained in single-spot laser welding. The aforesaid difference in quality could be ascribed to various energies supplied by the laser beam during twin-spot laser welding. Specimen 1 and 3 were made using the same welding linear energy, yet in the case of the twin-spot beam, the above named energy was the total energy of both beams.

Considering both beams separately led to the conclusion that, during welding, the first beam affected the steel with energy by half lower than the total energy. In such a case, the thermal effect on the material was less dynamic, which prevented weld face and weld root imperfections. In addition, the second beam remelted the previously formed weld affecting its macro- and microstructure. The welding process was performed in argon atmosphere. Keskitalo et al. [21] reported that the use of argon as the shielding gas improved the quality of welded joints.

The macrostructures made it possible to measure the widths of the individual zones of the weld. The measurement results are presented in Figure 2. The curves of width changes revealed that the use of twin-spot laser welding significantly widened both the fusion zone and the HAZ. In both cases it was observed that the increase in welding linear energy increased the width of both zones. However, it was also noticed that the increase in width related to twin-spot laser welding was significantly greater than that obtained in single-spot laser beam welding.

As regards the fusion zone, the increase in the width amounted to 0.05 mm in relation to single-spot laser welding, and 0.3 mm in relation to twin-spot welding. As regards the HAZ, the increase in the width amounted to 0.05 mm (similar to that of the fusion zone). The increase in the HAZ width related to twin-spot

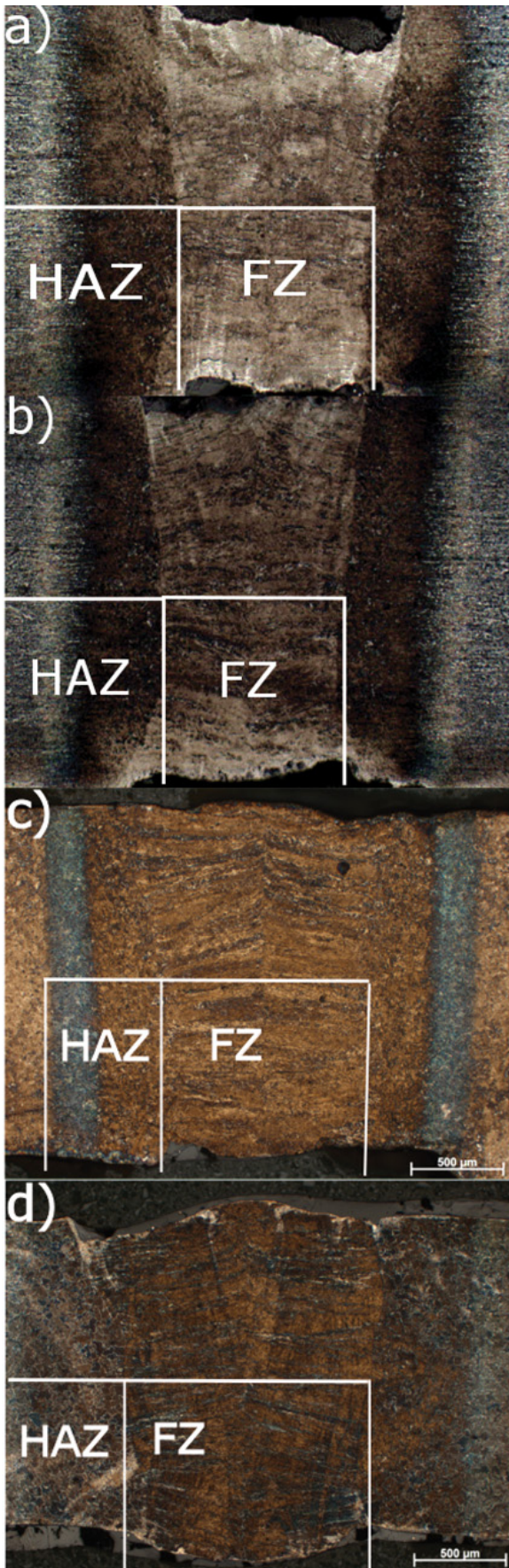


Fig. 1. Macrostructures of the joints made using: a), b) single-spot laser welding having a linear energy of 0.048 and 0.053 kJ/mm, respectively; c), d) twin-spot laser welding having a linear energy of 0.048 and 0.060 kJ/mm, respectively

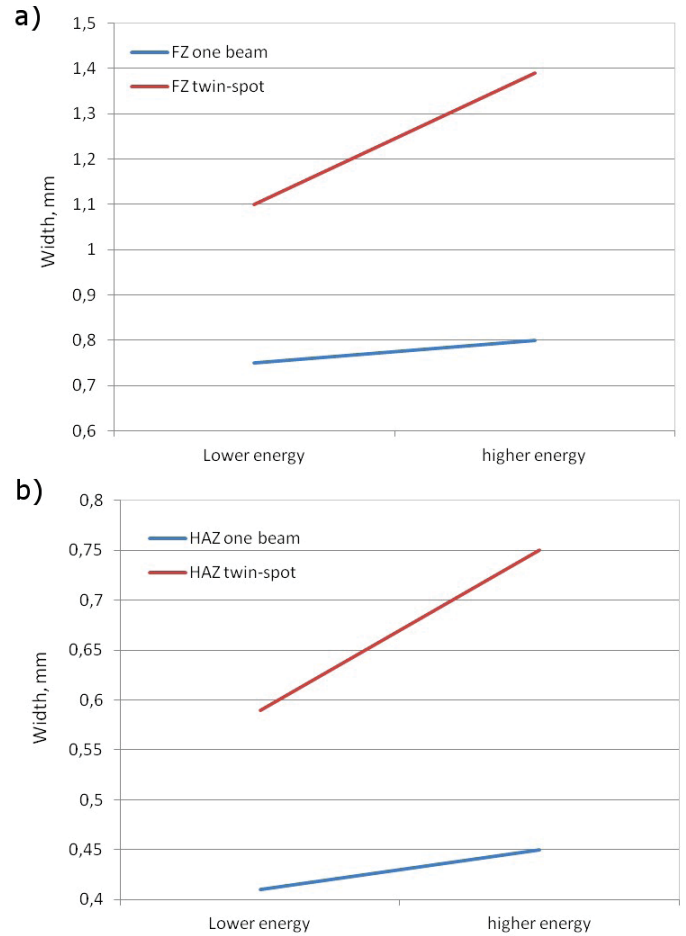


Fig. 2. Difference between the fusion zone width (a) and the HAZ width (b) in relation to single and twin-spot laser welding using various linear energy values

laser welding was significantly greater and amounted to 0.17 mm. The comparison of the above-presented results revealed that in spite of the similar values of welding linear energy, the beam effect in both welding techniques was different. This could be ascribed to the use of the second beam, which, by supplying additional heat input, reduced the cooling rate.

4.2. Microstructure investigations

The next stage of investigations involved the microstructural analysis of the base material and of the welded joint. The analysis was primarily focused on the fusion zone, heat affected zone and the transition zone between the base material and the HAZ. The SEM microstructure of the base material of steel TRIP is presented in Figure 3. As can be seen, the base material constitutes the fine-grained mixture of ferrite, bainite, retained austenite as well as contains bainitic-austenitic (BA) areas and martensitic-austenitic (MA) islands.

The microstructure of the fusion zone obtained using single- and twin-spot beam welding is presented in Figure 4. As can be seen in Figure 4a and 4b, the microstructure of the fusion zone welded using the single-spot beam was composed of lath

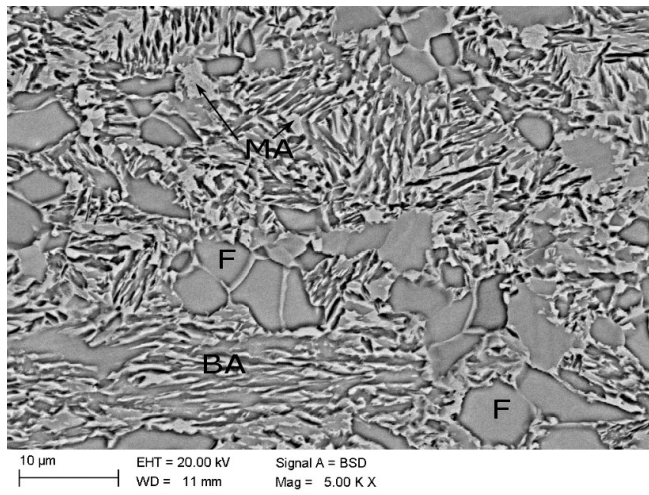


Fig. 3. Microstructure of the base material; F-ferrite, BA-bainitic-austenitic regions, MA-martensitic-austenitic islands

martensite and non-metallic inclusions. As regards twin-spot laser welding (Fig. 4c and 4d), the microstructure was, similar to single-spot welding, composed of lath martensite. In contrast to the microstructure made using single-spot laser welding, the martensite laths in the microstructure made using twin-spot laser welding was characterised by greater dispersion, which could indicate the initiation of tempering-like processes. Similar to the microstructure made using single-spot laser welding, the microstructure made using twin-spot laser welding contained non-metallic inclusions.

The presence of non-metallic inclusions when welding steel TRIP in the atmosphere of air and argon was explained by Grajcar et al. [17]. They reported that the use of argon as the shielding gas during laser welding led to the slight reduction of non-metallic inclusions. This was caused by the formation of a strong gas stream and metal vapours due to high power emitted during keyhole welding. The gas stream penetrated the atmosphere of argon enabling the access of air to liquid metal. The presence of non-metallic inclusions in the fusion zone is considered to be unfavourable. Zork et al. [22] found that the presence of significant amounts of non-metallic inclusions in the fusion zone could result in hot cracking. As regards the steel subjected to analysis, none of the welding variants used in the tests was accompanied by crack formation in the joint material.

The morphological details of the fusion zone related to the use of twin-spot laser beam welding are presented in Figure 5. As can be seen in the SEM image, the fusion zone, in addition to martensite, contains the small amount of retained austenite located along the martensite laths and on the edges of the MA-type grains. Kobayashi et al. [23] also revealed the presence of retained austenite films between martensite laths in the fusion zone of 0.2C-1.5Mn-1.5Si type TRIP steel. A certain content of retained austenite in the microstructure of the fusion zone of laser welded TRIP steel was also identified by Zhao et al. [24] who stated that the use of welding techniques enabling the reduction of cooling rates enriched austenite in carbon thus increasing its temperature stability. The results obtained in the tests confirmed

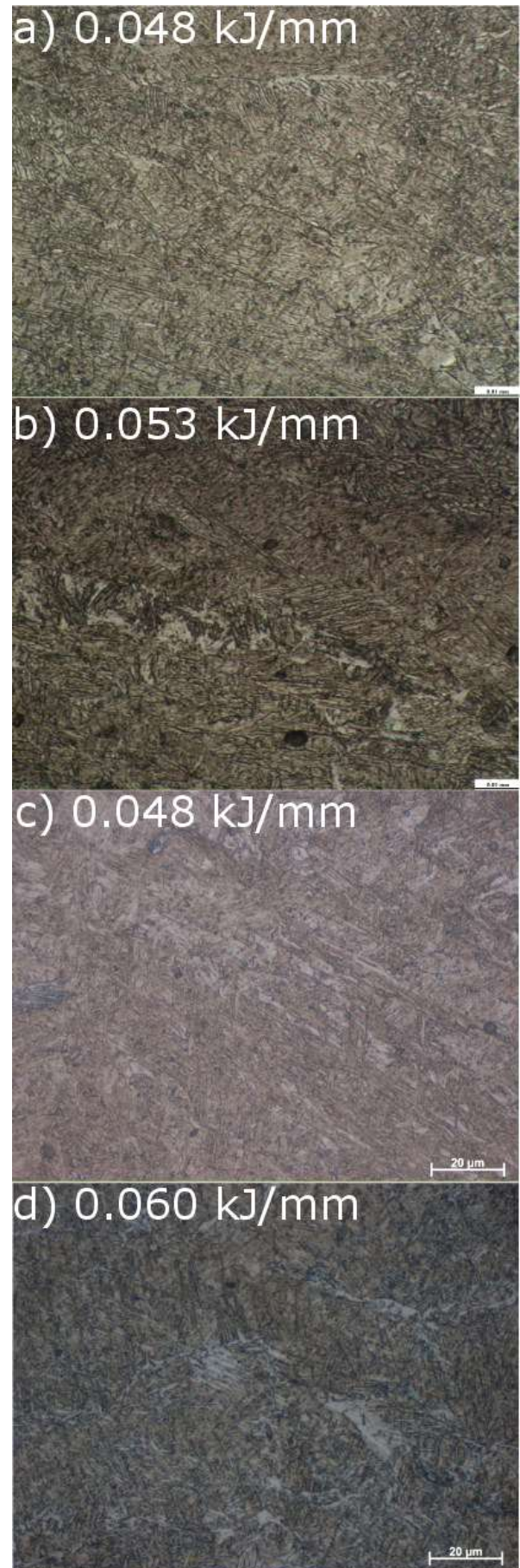


Fig. 4. Microstructure of the fusion zone subjected to: a), b) single-spot laser beam welding, c), d) twin-spot laser beam welding

the above statement; twin-spot laser welding is characterised by slower cooling rates in comparison with conventional laser welding.

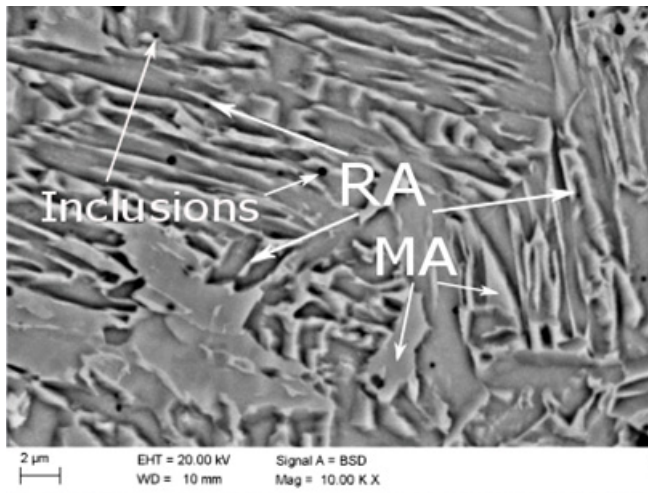


Fig. 5. Microstructure of the fusion zone in steel TRIP subjected to twin-spot laser welding

The microstructure of the heat affected zone subjected to single and twin-spot laser beam welding was composed of the fine-grained mixture of bainite and martensite (Fig. 6). The SEM microphotographs revealed the presence of retained austenite as regards both single and twin-spot laser welding. The clear boundary between fine-grained and coarse-grained microstructure can be visible in Figure 7a. The retained austenite was present in bainite and on the edges of martensitic packets. Zhao at al. [24] reported that retained austenite favourably affected steel weldability as it prevented the propagation of cracks formed during exposure to loads. Twin-spot laser beam welding is responsible for the defragmentation of martensite, which implies the occurrence of tempering-like processes (Fig. 7b). The resulting reduction of hardness should positively affect properties of welded joints by reducing their crack susceptibility. The content of non-metallic inclusions was significantly smaller when compared to the fusion zone.

The last zone subjected to metallographic analysis was the transition zone between the base material and the HAZ. The analysis revealed that the transition zone contained the mixture of ferrite, bainite, martensite and retained austenite. The content of ferrite grew as the distance to the base material became shorter. Figure 8 presents the microstructure of the transition zone subjected to single (Fig. 8a,b) and twin-spot laser welding (Fig. 8c,d). As can be seen, the transition zone was visible better if welded using the single-spot laser beam.

The analysis of Figure 9 presenting the microstructure of the transition zone at a higher magnification revealed that the use of the single-spot beam led to the presence of retained austenite in the IC-HAZ, on the edges of martensite laths and in the form of single fine bright grains. A similar tendency was also observed when the twin-spot laser beam was used. As regards single-spot and twin-spot welding, the fusion zone was characterised by



Fig. 6. Microstructure of the heat affected zone of steel TRIP subjected to: a), b) single-spot laser beam welding, c), d) twin-spot laser beam welding

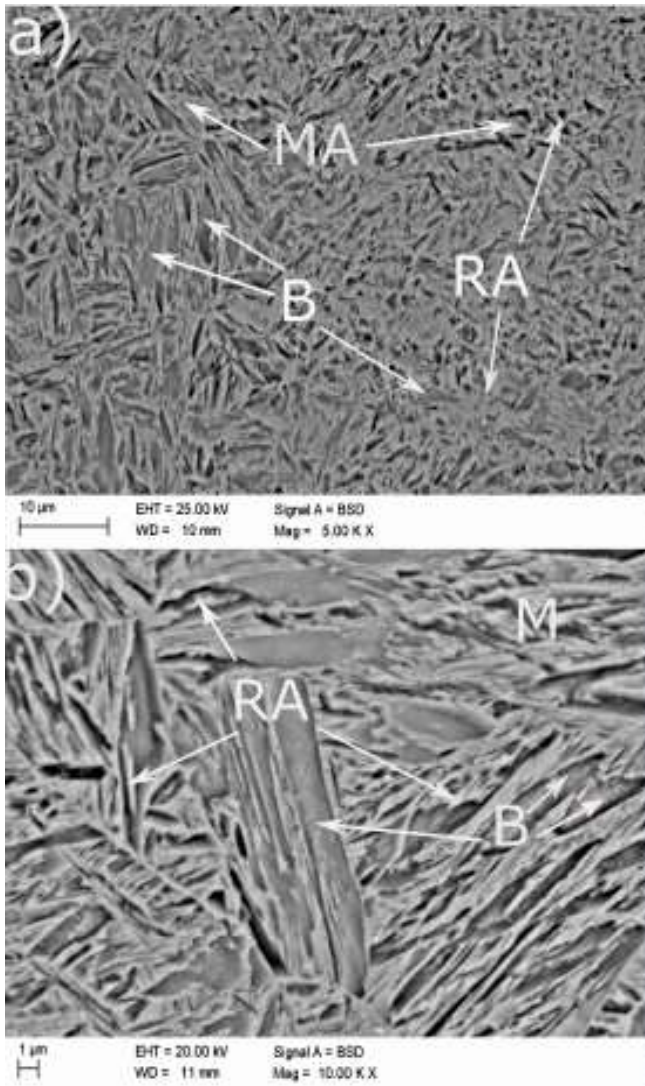


Fig. 7. SEM microphotographs presenting the microstructure of the HAZ in relation to: a) single-spot laser beam welding, b) twin-spot laser beam welding

blocky-like morphology dominated by martensite. However, in twin-spot laser welding (Fig. 9b), martensite was more defragmented due to a longer time during which the material being welded was exposed to the effect of the laser beam. The content of retained austenite was greater than both in the fusion zone and in the HAZ as a result of a partial carbon partitioning between α phase and austenite. This behaviour was similar in both single and twin-spot laser welded specimens.

4.3. Hardness

In order to determine the quality of the single and twin-spot laser welded joints it was necessary to measure their hardness. The results of hardness measurements are presented in Figure 10. As regards single-spot laser welding, the hardness of the fusion zone was similar for both values of linear energy and amounted to app. 486 HV. In turn, in the case of twin-spot laser welding, the average value of hardness amounted to 443 HV. The decrease in

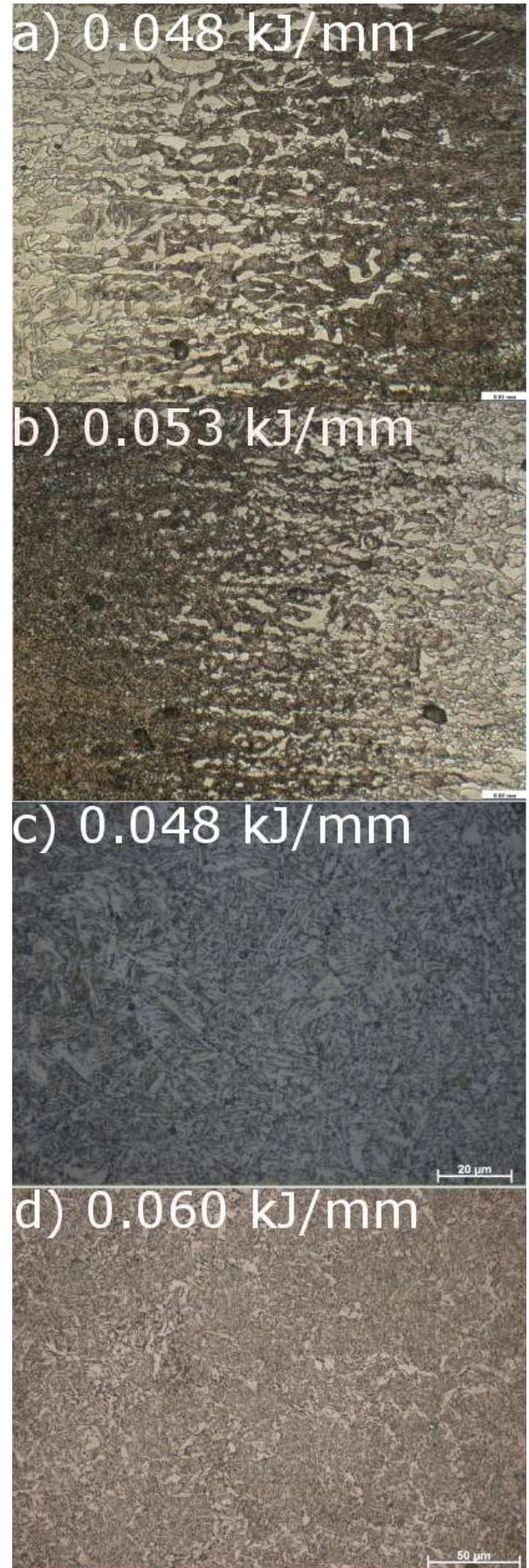


Fig. 8. Microstructure of the transition zone between the base material and the HAZ: a), b) single-spot laser beam welding, c), d), twin-spot laser beam welding

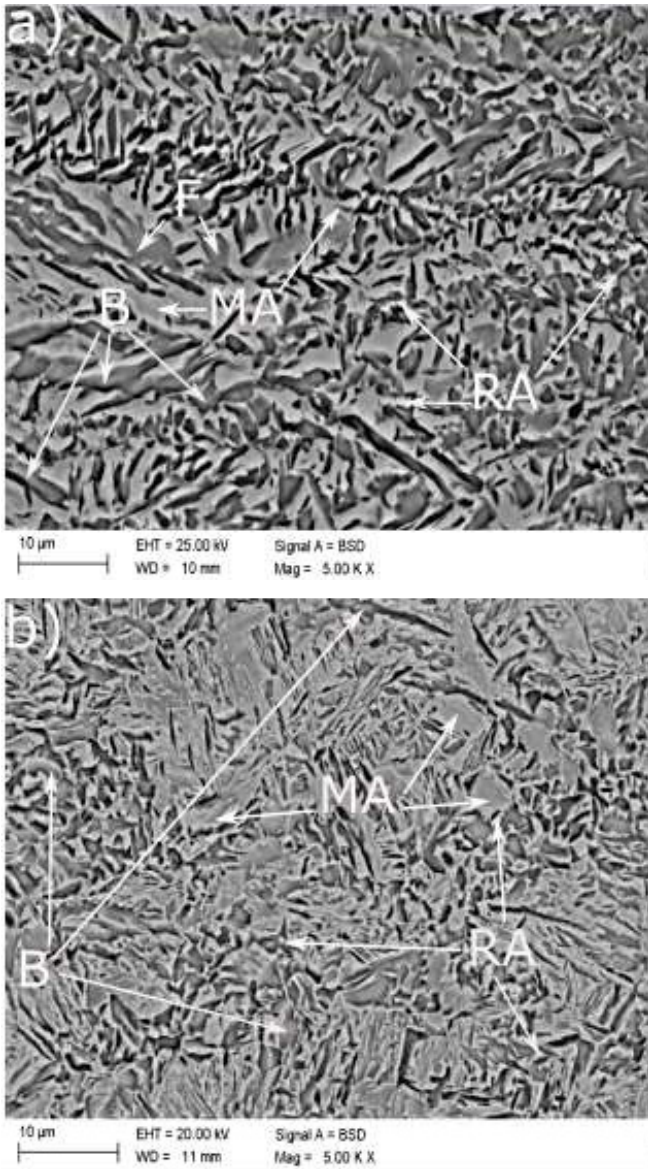


Fig. 9. Microstructure of the transition zone obtained during the SEM observation: a) single-spot laser beam welding, b) twin-spot laser beam welding

the fusion zone hardness could be ascribed to the influence of the second beam responsible for the defragmentation of martensite through the partial initiation of diffusional processes. A similar tendency was observed in the heat affected zone. The hardness obtained in single-spot laser welding amounted to approximately 520HV, whereas that obtained in twin-spot laser welding amounted to 480HV. Similar to the fusion zone, the reason for such a situation was the defragmentation of martensite caused by the decrease in thermal cycle dynamics induced by the second beam. As can be seen, the use of the second beam influencing the microstructure of the material being welded positively affected its hardness.

5. Summary

The use of twin-spot laser welding affects both the hardness and the microstructure of materials being welded. If compared to single-spot laser welding, twin-spot laser welding is characterised by the following features:

- by reducing the dynamics of welding thermal cycles (greater heat input to a material being welded), twin-spot laser welding facilitates the occurrence of tempering-like processes,
- unlike joints made using single-spot laser welding, twin-spot laser welded joints are free from weld face and weld root imperfections,
- due to the greater heat input accompanying the use of twin-spot laser welding, the width of the fusion zone and that of the HAZ are greater than those obtained during single-spot laser welding using the same linear energy,
- tempering triggered by the second beam leads to the defragmentation of martensite,
- some fraction of retained austenite is thermally stable after laser welding cycles in the intercritical heat-affected zone,
- twin-spot laser welding reduces the hardness of the analysed TRIP steel by approximately 40 HV in the fusion zone and in the HAZ.

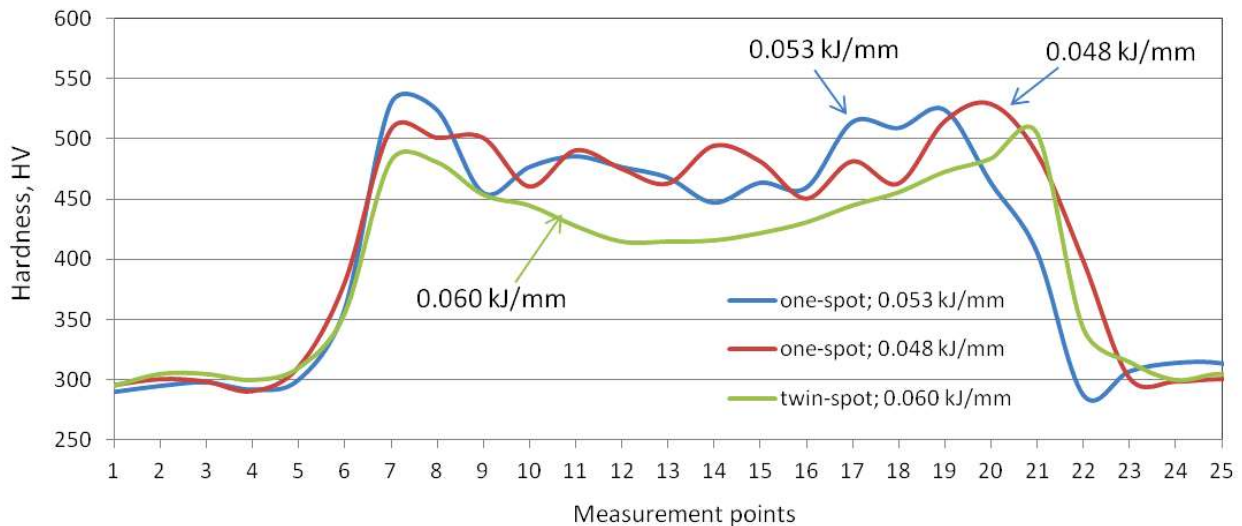


Fig. 10. Hardness profiles through the fusion zone, HAZ, IC-HAZ and base metal for single-spot and twin-spot laser beam welding

Acknowledgment

This work was financially supported with statutory funds of Faculty of Mechanical Engineering of Silesian University of Technology in 2016.

REFERENCES

- [1] A. Lisiecki, *Metals* **5** (1), 54-69 (2015).
- [2] D.M. Janicki, *Solid State Phenom.* **199**, 587-592 (2013).
- [3] Y. Miyashita, *Handbook of laser welding technologies*, chapter 16: Developments in twin-beam laser welding technology, 2013.
- [4] J. Milberg, A. Trautmann, *Production Process: Research and Development* **3** (1), 9-15 (2009).
- [5] W. Chen, P. Molian, *Int. J. Adv. Manuf. Technol.* **39**, 889-897 (2008).
- [6] S. Pang, W. Chen, J. Zhou, D. Liao, *J. Mater. Proc. Technol.* **217**, 131-143 (2015).
- [7] A. Kokosza, J. Pacyna, *Mater. Sci. Technol.* **33** (7), 802-807 (2015).
- [8] R. Blonde, E. Jimenez-Melero, L. Zhao, J.P. Wright, E. Bruck, S. van der Zwaag, N.H. van Dijk, *Mater. Sci. Eng. A* **618**, 280-287 (2014).
- [9] L.A. Dobrzański, M. Czaja, W. Borek, K. Labisz, T. Tański, *Int. J. Mater. Prod. Tech.* **51** (3), 264-280 (2015).
- [10] A. Grajcar, K. Radwański, H. Krztoń, *Solid State Phenom.* **203-204**, 34-37 (2013).
- [11] M. Jabłońska, R. Michalik, *Solid State Phenom.* **227**, 109-112 (2015).
- [12] E. Skolek, K. Wasiak, W.A. Świątnicki, *Mater. Tehnol.* **49** (6), 933-939 (2015).
- [13] M. Dziedzic, S. Turczyn, *Arch. Civ. Mech. Eng.* **10**, 21-30 (2010).
- [14] M.S. Weglowski, S. Stano, G. Michta, W. Osuch, *Arch. Metall. Mater.* **55**, 211-220 (2010).
- [15] A. Grajcar, M. Róžański, S. Stano, A. Kowalski, B. Grzegorzczak, *Adv. Mater. Sci. Eng.* **2014**, 8 pages, doi.org/10.1155/2014/658947 (2014).
- [16] A. Grajcar, M. Róžański, S. Stano, A. Kowalski, *J. Mater. Eng. Perform.* **23**, 3400-3406 (2014).
- [17] A. Grajcar, M. Róžański, M. Kamińska, B. Grzegorzczak, *Mater. Tehnol.* **50** (6), 945-950 (2016).
- [18] J. Górka, *Indian J. Eng. Mater. Sci.* **22**(5), 497-502 (2015).
- [19] M. Opiela, *Mater. Tehnol.* **49** (3), 395-401 (2015).
- [20] K. Radwański, *Steel Res. Int.* **86** (11), 1379-1390 (2015).
- [21] M. Kaskitalo, J. Sundqvist, K. Mantyjärvi, J. Powell, A.F.K. Kaplan, *Physics Proc.* **78**, 222-229 (2015).
- [22] B. Zorc, M. Imamovic, L. Kosec, B. Kosec, A. Nagode, *Mater. Tehnol.* **48** (1), 149-154 (2014).
- [23] J. Kobayashi, S.M. Song, K. Sugimoto, *ISIJ Int.* **52** (6), 1124-1129 (2012).
- [24] L. Zhao, M.K. Wibowo, M.J.M. Hermans, S.M.C. van Bohemen, J. Sietsma, *J. Mater. Proc. Technol.* **209**, 5286-5292 (2009).